

Z Cha and its Superhumps

J. S m a k

N. Copernicus Astronomical Center, Polish Academy of Sciences,
Bartycka 18, 00-716 Warsaw, Poland
e-mail: jis@camk.edu.pl

Received

ABSTRACT

The superhump eclipse light curves are re-determined for five eclipses of Z Cha (E54036, E54037, E67877, E74693, E74694) observed by Warner and O'Donoghue (1988) during its superoutbursts. Qualitatively they are similar to those obtained by O'Donoghue (1990), showing two local minima at $\phi \sim -0.05$ and 0.04. Arguments are then presented which imply that the first minimum is not due to an occultation but is produced by absorption effects in the overflowing parts of the stream. The location of the superhump light source (SLS) determined from the analysis of the second minimum coincides with the trajectory of the overflowing parts of the stream.

The light curve of the sixth eclipse (E77878) could be simply decomposed into its disk and superhump components. The location of SLS, obtained from the analysis of the SLS eclipse light curve, coincides in this case with the position of the standard hot spot.

This implies that superhumps are due to modulated mass transfer rate resulting in periodically enhanced dissipation of the kinetic energy of the stream.

Key words: *accretion, accretion disks – binaries: cataclysmic variables, stars: dwarf novae, stars: individual: Z Cha*

1. Introduction

This is the third paper in a series devoted to the analysis of light curves of Z Cha observed during its superoutbursts by Warner and O'Donoghue (1988). In the first paper (Smak 2007) the light curves covering eclipses located away from superhumps were decomposed into their disk eclipse and hot spot eclipse components. In the second paper (Smak 2008) the accretion rates, determined from disk eclipse analysis, were found to be practically identical with the mass transfer rates determined from spot luminosities, what implies that superoutbursts are due to a major enhancement in the mass transfer rate. In the present paper we analyze eclipses at beat phases near $\phi_b \sim 0$, i.e. those which involve the occultation of the superhump light source.

The first such analysis was made by Warner and O'Donoghue (1988) who applied the Maximum Entropy Method (MEM) to two eclipses involving superhumps: E54037 and E77878. In the first case the superhump light source (SLS) was identified by them with a peak in the resulting "MEM image", located near the edge of the disk and facing the secondary component (i.e. not far from the location of the standard hot spot). In the case of E77878 they found the location of SLS to be "*consistent with a position on the edge of the disk beginning at the quiescent bright spot and continuing downstream*" or "*along the continuation of the stream into the inner disc*". In spite of that, however, Warner and O'Donoghue concluded that those results "*eliminate locations in the vicinity of the quiescent bright spot or along the mass-stream*"...

Two years later O'Donoghue (1990), using also the MEM technique, made a more detailed analysis of four superhump eclipses. His "MEM images" for E54036, E54037, and E67877 showed that the superhump light source (SLS) consists of three distinct areas: area 1 – on the trailing lobe of the disk, area 2 – on its leading lobe, and area 3 – near the edge of the disk, facing the secondary component. This was interpreted by O'Donoghue (and emphasized in the title of his paper) as the observational evidence for the tidal origin of superhumps. This interpretation, however, encounters one serious problem. Contrary to the statements by O'Donoghue that "*the superhump light source is located on the rim of the disk*" and that this "*strongly suggests that tidal stresses are responsible*", one can easily see from his "MEM images" that the centers of area 1 and area 2 are located at $r/r_d \approx 0.5 - 0.6$ (where $r_d = r_{tid} = 0.9r_{Roche}$), i.e. roughly half-way between disk edge and its center. In addition, there was the case of E77878 showing – as before – that SLS consists of only one area located "*very close to the position of the bright spot at quiescence*".

Those discrepancies suggested that another, independent analysis of the problem should be undertaken. In Section 2 we substantially modify the method used earlier by O'Donoghue to obtain the superhump eclipse light curves and present the resulting new light curves for five eclipses (E54036, E54037, E67877, E74693, and E74694). They are qualitatively similar to those obtained by O'Donoghue, showing two local minima at $\phi \sim -0.05$ and $\phi \sim 0.04$. Evidence is then presented (Sections 3 and 4) which implies that the first minimum is produced by absorption effects in the overflowing parts of the stream. From the analysis of the second minimum (Section 5) we find that the location of SLS coincides with the trajectory of the overflowing parts of the stream. In Section 6, devoted to the sixth eclipse E77878, we simply decompose its observed light curve into the disk and superhump components and find that in this case the location of SLS coincides with the position of the standard hot spot. Using this evidence we conclude (Section 7) that (1) superhumps are due to periodically enhanced dissipation of the kinetic energy of the stream resulting from strongly modulated mass transfer rate and (2) substantial stream overflow occurs around superhump maximum making the superhump

light source similar to "peculiar" spots observed at intermediate beat phases.

2. The Light Curves of Superhumps

O'Donoghue (1990) analyzed five eclipses (E54036, E54037, E67877, E74693 and E77878) involving superhumps using the following simple method. The superhump eclipse light curve was determined as

$$\ell_{sh} = \ell_{obs}(d) - \ell_{obs}(d-1), \quad (1)$$

where $\ell_{obs}(d)$ is the eclipse light curve under analysis and $\ell_{obs}(d-1)$ – the eclipse light curve observed on the previous night, when the eclipse was located away from superhumps. The out-of-eclipse superhump light curve ℓ_{sh}° was assumed to be identical with that observed also on the previous night. The resulting superhump eclipse light curves (Figs.1-7 in O'Donoghue 1990) showed two local minima: one near $\phi \sim -0.05$, and another at $\phi \sim 0.05$, and a local maximum between them near $\phi \sim 0.0$.

The method used by O'Donoghue suffered from his arbitrary assumption that the light curves observed on the previous night are representative for the situation under analysis. This is not the case. First of all, the observed depth of eclipse increases with time (see Fig.6 in Warner and O'Donoghue 1988). Secondly, the eclipse light curve observed on the previous night (away from superhump) consists of the disk and spot components, the contribution from the spot depending strongly on the superhump phase (cf. Smak 2007). Thirdly, the superhump amplitude is also not constant: it decreases with time (see Fig.5 in Warner and O'Donoghue 1988).

In the present analysis we modify the method used by O'Donoghue in several ways. To begin with, we determine the superhump eclipse light curve as

$$\ell_{sh} = \ell_{obs} - \ell_d, \quad (2)$$

where ℓ_d is the pure disk eclipse curve. As shown earlier (Smak 2008, Fig.1), the depth of disk eclipse $\Delta\ell_d$ increases with time. Rewriting Eq.(1) from that paper we have

$$\Delta\ell_d = 0.494 + 0.050 \Delta t, \quad (3)$$

where Δt is the time (in days) since the beginning of superoutburst. To check whether the shapes of disk eclipse light curves differ also in some other way, we reduce all disk light curves obtained earlier from eclipses observed at beat phases $0.4 < \phi_b < 0.6$ (Smak 2007) to an arbitrarily adopted central intensity $\ell_o = 0.50$. Results, presented in Fig.1, show that the shapes of eclipses normalized in such a way are practically identical. This mean reduced disk light curve together with $\Delta\ell_d$ from Eq.(3) can then be used to calculate the disk light curve applicable via Eq.(2) to the situation considered.

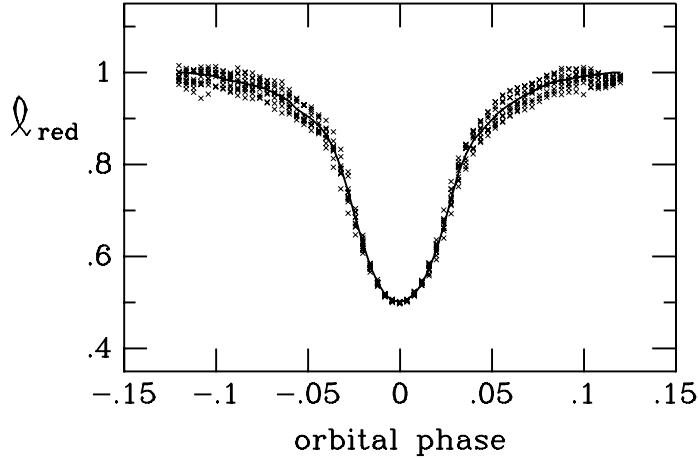


Fig. 1. Disk eclipse light curves reduced to central intensity $\ell_o = 0.5$. Solid line is the mean reduced curve.

To obtain the normalized superhump light curve

$$\ell_{sh}^n = \ell_{sh} / \ell_{sh}^\circ \quad (4)$$

we need the out-of-eclipse superhump light curve ℓ_{sh}° . This step introduces some uncertainty. In addition to the already mentioned dependence of the superhump amplitude on Δt , their shapes vary considerably from one superhump to another showing, in particular, large scale rapid flickering. After analyzing superhump light curves from Warner and O'Donoghue (1988) it was found (in agreement with a similar conclusion by O'Donoghue 1990) that their shapes can be – approximately – represented by

$$\ell_{sh}^\circ(\phi) = A_{sh} \exp [-a(\phi - \phi_{max})^2], \quad (5)$$

or, to account for their frequent asymmetry, by

$$\ell_{sh}^\circ(\phi) = A_{sh} \exp [-a(\phi - \phi_{max})^2 - b(\phi - \phi_{max})^3], \quad (6)$$

where A_{sh} is the superhump amplitude and ϕ_{max} – the phase of its maximum. Depending on the situation (see below) one of these two formulae was fitted to the out-of-eclipse parts of the observed superhump light curves.

In this Section we present results for five eclipses, namely: E54036, E54037, E67877, E74693 and E74694 (not analyzed by O'Donoghue). In the first two cases, with superhump maximum occurring within the eclipse, we use Eq.(6) with $A_{sh} = 0.35$ (from Fig.5 of Warner and O'Donoghue 1988), ϕ_{max} from the superhump ephemeris, and determine the two remaining unknown parameters: a and b . In the three other cases, with superhump maximum occurring just before the eclipse, we use Eq.(5) and determine all three parameters: A_{sh} , ϕ_{max} and a .

Results are presented in Figs.2-4. As can be seen our superhump light curves are qualitatively similar to those of O'Donoghue: they show two local minima at $\phi \sim -0.05$ and $\phi \sim 0.04$, and a local maximum near $\phi \sim -0.01$.

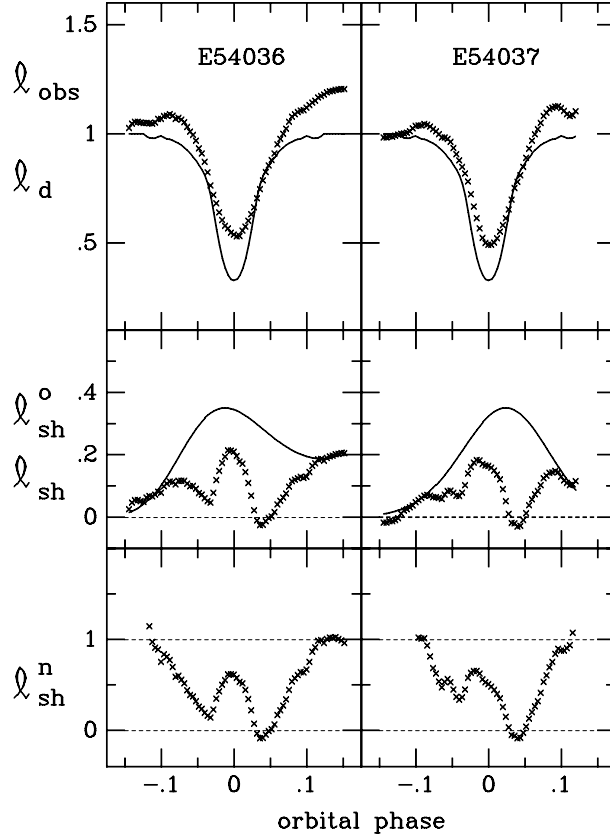


Fig. 2. Light curve analysis for eclipses E54036 and E54037. Shown with crosses are the observed light curves (*top*), the superhump light curves (*middle*), and the normalized superhump light curves (*bottom*). Shown with solid lines are the disk light curves (*top*) and the fitted out-of-eclipse superhump light curves (*middle*).

The case of E74694 (not analyzed by O'Donoghue) requires special comments. The locations and depths of the two local minima are similar to other cases but the local maximum at $\phi \sim -0.01$ reaches an unacceptable value of $\ell_{sh}^n(\max) \approx 1.9$. In an attempt to explain its origin we repeated our analysis using slightly modified input parameters. The right panel of Fig.4 shows an example of such a modification in which the observed light curve was corrected by adopting "level 1" at $\ell = 0.95$ and the disk light curve was made shallower by 10 percent (both these changes being acceptable within existing uncertainties). As one can see, those modifications resulted in a much lower height of the local maximum (the shape of the two minima remaining roughly the same). In view of the arbitrary nature of

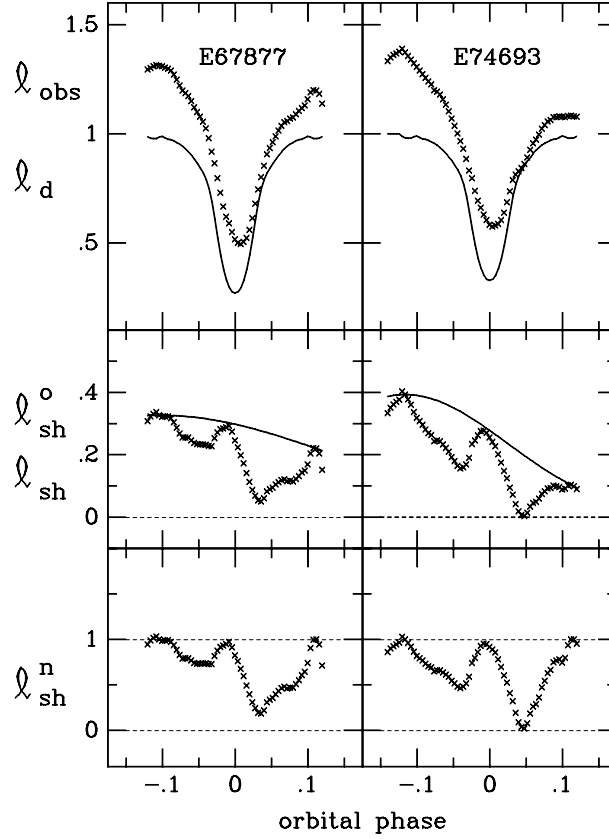


Fig. 3. Light curve analysis for eclipses E67877 and E74693 (see caption to Fig.2).

such modifications, however, no attempt was made to continue such experiments until getting $\ell_{sh}^n(\max) = 1$.

Turning to a more detailed comparison of our superhump light curves with those obtained by O'Donoghue, we note significant difference with respect to the second minimum (at $\phi \sim 0.04$) which in our case is much deeper: the four light curves of O'Donoghue (excluding E77878) give the mean depth of $\langle \Delta\ell \rangle \approx 0.8$, while our five light curves give $\langle \Delta\ell \rangle \approx 1.0$. There are also other differences. In the case of E67877 the local maximum around $\phi \sim -0.01$ obtained by O'Donoghue reached only $\ell_{sh}^n \approx 0.7$, while in our case $\ell_{sh}^n \approx 1.0$. In the case of eclipse E74693 O'Donoghue encountered problem similar to our problem with E74694: his local maximum around $\phi \sim -0.01$ exceeded "level 1". Our analysis of this eclipse removed this problem giving $\ell_{sh}^n \approx 1.0$.

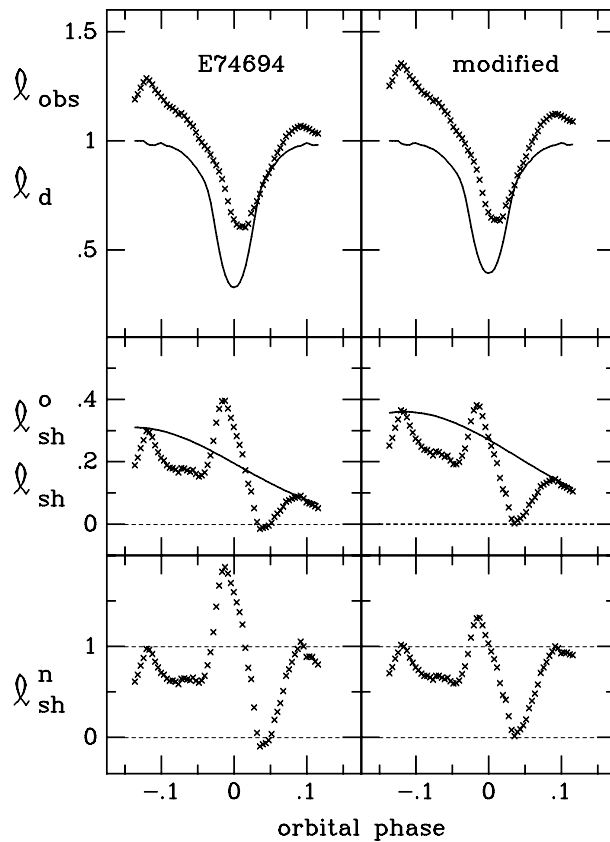


Fig. 4. Light curve analysis for the eclipse E74694 (see caption to Fig.2). The left panel shows the standard analysis while the right panel – its modification, as discussed in the text.

3. Are We Dealing with Pure Eclipses?

In the standard analysis of eclipse light curves they are used to determine the surface brightness distribution over the surface of the disk. O'Donoghue (1990) did this using the Maximum Entropy Method (MEM). From the very nature of the MEM technique one could expect the model light curves calculated from the "best MEM image" to provide perfect fit to the observed eclipse light curves. However, as can be seen from Figs.1-5 of O'Donoghue's, all his model light curves show minima which are too shallow by as much as 10-20 percent. Obviously then something must have been wrong...

In our analysis we used a much simpler and more straightforward method: The disk was divided into $6 \times 6 = 36$ square areas and their surface brightnesses (x_i , $i = 1, 36$) were determined by a formal least-squares fit to the observed light curve. In all cases analyzed the results were dramatically disappointing: roughly one-third of the resulting values of x_i (particularly those on the leading lune of the disk) turned out to be negative or strongly negative! Again, obviously, something must have

been wrong...

To identify the nature of those problems let us take a closer look at the light curves. As mentioned above, the mean depth of the second minimum at $\phi \approx 0.04$ is $\langle \Delta\ell \rangle \approx 1.0$ what means that the superhump light source (SLS) is fully eclipsed at that phase. The relatively narrow shape of this minimum and its central phase imply that SLS must be rather small and located somewhere on the trailing lobe of the disk. If so, the first minimum, at $\phi \approx -0.05$, cannot be due to another occultation of SLS at that phase...

Our arguments become even more straightforward in the case of eclipses E67877, E74693, and E74694. At $\phi \approx -0.01$ their light curves (Figs.3 and 4) show $\ell_{sh}^n \approx 1$. This could imply that the two minima represent two separate eclipses of two parts of SLS. If so, their normalized depths should obey the obvious condition: $\Delta\ell_1 + \Delta\ell_2 \leq 1$. In fact, however, in the case of those three eclipses we have, respectively, $\Delta\ell_1 + \Delta\ell_2 \approx 1.1, 1.5,$ and 1.4 . This means that they cannot be due only to an occultation of SLS by the secondary component. In other words – that one of the two minima (or both) must be partly due to some other effect(s). This explains why previous attempts to analyze those light curves by treating them as pure eclipses encountered problems discussed above.

4. The Case for Absorption Effects

Listed below are facts and arguments which consistently suggest that problems described above have their source in absorption effects. Specifically – that the first minimum is caused by absorption in the overflowing parts of the stream.

(1) The evidence for a substantial stream overflow in Z Cha during its superoutbursts came from the analysis of "peculiar" spot eclipses observed at intermediate beat phases away from $\phi_b \sim 0.5$ (Smak 2007). The spot distances obtained from those eclipses turned out to be smaller than the radius of the disk, indicating that such "peculiar" spots are formed partly in the overflowing parts of the stream.

The stream overflow was originally expected to occur only when the disk is geometrically thin, i.e. mainly in quiescent dwarf novae (cf. Hessman 1999 and references therein). In addition to the observational evidence quoted above, however, there is also theoretical evidence (Kunze et al. 2001) suggesting that it is a much more common phenomenon.

(2) Fig.5-*left* shows the view of the system at $\phi = -0.05$. It can immediately be seen that around that phase the overflowing portions of the stream pass between the observer and the center of the disk and therefore are likely to absorb part of the flux coming from its central (brightest) parts. On the other hand, Fig.5-*right* shows that no major effects of this type should be present around the second minimum at $\phi = 0.04$ simply because the stream and the adjacent portions of the disk are fully eclipsed at that phase.

The effective optical depth of the absorbing material can be estimated from:

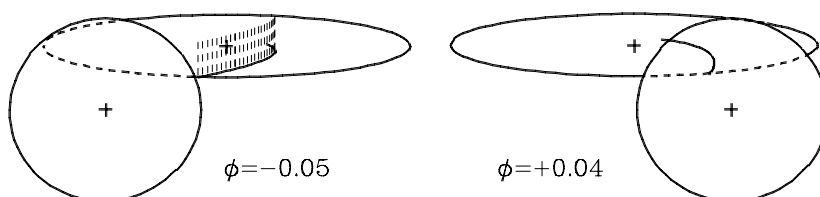


Fig. 5. View of Z Cha at $\phi = -0.05$ (left) and $\phi = 0.04$ (right). Solid lines show the disk, the secondary, and the stream trajectory in the orbital plane ($z = 0$). Short dashed lines in the left picture show the vertical extent ($z = 0.1$, assumed) of the overflowing parts of the stream.

$$\tau = \ln \left(\frac{\xi \ell_d - \Delta \ell_{sh} \ell_{sh}^{\circ}}{\xi \ell_d} \right), \quad (7)$$

where $\Delta \ell_{sh}$ is the depth of the first minimum at $\phi = -0.05$, ℓ_{sh}° – the out-of-eclipse luminosity (in intensity units normalized to "level 1"), ℓ_d – the luminosity of the disk at that phase, and ξ – its effective fraction affected by absorption. Using values of the relevant parameters taken from Figs.2 and 3 and assuming $\xi = 0.5$ we get a range of $\tau \approx 0.2 - 1.6$ which shows that relatively little material is needed to produce the observed effects.

(3) The idea of absorption effects being produced in the overflowing parts of the stream is not new. The first evidence for such effects came from the analysis of "peculiar" spot eclipses (Smak 2007) where it was found that spot distances obtained from ingress r_i are systematically larger than those obtained from egress r_e . This was interpreted as being due to selfabsorption in the overflowing parts of the stream: during ingress, when the stream trajectory is nearly parallel to the line of sight, the effective light center of the "peculiar" spot is observed closer to the disk edge.

Two additional effects supporting this interpretation can be predicted. To do so let us recall some details of the method which was used to decompose the observed light curves into their disk and spot components (Smak 1994, 2007). In step 2, involving crucial assumption that the disk eclipse light curve is symmetric around phase zero, the spot light curve is determined in the phase interval $[-\phi_3, -\phi_2]$. Worth noting is that the values of ℓ_s for $\phi < \phi_1$, representing its uneclipsed portion, are essential for determining the spot amplitude A_s . Let us now consider the situation when absorption effects of the type discussed above are present, affecting the shape of the disk eclipse light curve at negative phases around $\phi \sim -0.05$. Since we now have $\ell_d(\phi < 0) < \ell_d(\phi > 0)$ the resulting values of $\ell_s(\phi < 0)$ will come out lower by $\Delta \ell_s = \ell_d(\phi > 0) - \ell_d(\phi < 0)$, causing the resulting spot amplitude A_s to be also lower. Turning to the observational evidence we recall that spot amplitudes determined from "peculiar" spot eclipses (Smak 2007, Fig.5) are indeed systematically lower.

Another effect can be predicted for the part of the spot light curve around $\phi = 0$, representing its total eclipse, where we normally have $\ell_s(\phi) \equiv 0$. In the case of

absorption effects, however, when $\ell_d(\phi < 0) < \ell_d(\phi > 0)$ we expect $d\ell_s/d\phi > 0$. Turning to the observational evidence and using the "standard" spot light curves we get $d\ell_s/d\phi = -0.08 \pm 0.06$. In the case of "peculiar" spot light curves, however, we obtain $d\ell_s/d\phi = +0.67 \pm 0.08$. (Worth adding is that this difference could be seen directly from Fig.1 in Smak (2007) showing three examples of "standard" spots and another three examples of "peculiar" spots).

5. The Location of the Superhump Light Source

As already mentioned earlier, no major absorption effects are to be expected in the case of the second minimum around $\phi \approx 0.04$. Therefore it can be treated as being mainly due to an occultation of the superhump light source (SLS). Taking into account, however, that some absorption effects may still contribute to its shape we do not attempt to analyze it in any formal way. Instead we limit ourselves to a qualitative analysis.

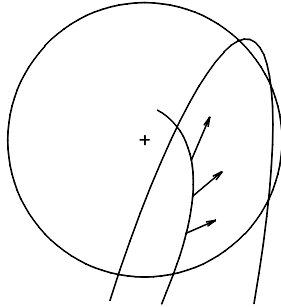


Fig. 6. Geometrical constraints on the location of SLS. Shown are: the disk and the limb of the secondary at $\phi = 0.04$ in projection on the orbital plane (broken lines). Solid line is the stream trajectory, while arrows represent the rotational velocity vectors of the disk. See text for details.

The geometry of eclipse at the central phase of the second minimum ($\phi = 0.04$) presented in Fig.6 shows that the eclipsed area includes the stream and the adjacent parts of the disk. At first sight the stream may appear not to be the best candidate since its trajectory is located asymmetrically with respect to the central line of the projected limb of the secondary. We should recall, however, that this trajectory was calculated without taking into account any interactions with the surface elements of the disk. It is obvious that due to those interactions the stream must be deflected in the direction of disk's rotation, as shown by arrows in Fig.6. Taking this into account we can conclude that the location of SLS actually coincides with the overflowing parts of the stream.

6. The Case of E77878

This eclipse was described by Warner and O'Donoghue as "*anomalous*" or "*extremely peculiar*". It appears that the only reason for such a classification was that results obtained from this eclipse (quoted in the Introduction) did not support their main conclusion about tidal origin of superhumps.

E77878 is, in fact, simpler and cleaner than other eclipses. To begin with, the superhump eclipse light curve (Fig.7 in O'Donoghue 1990) shows no trace of the first minimum around $\phi \sim -0.05$. This implies that the absorption effects (responsible for the first minimum observed in other cases) were absent. If so, it appeared reasonable to try to decompose the observed light curve into its disk and superhump component using the same simple method which was used earlier in the case of hot spots (Smak 2007). Results are shown in Fig.7. Filled squares represent points obtained in Steps 1 and 2 of the decomposition procedure (see Smak 1994). They are used to determine (using Eq.5) the "out-of-eclipse" superhump light curve (solid line), which is then used in Step 3 to determine the remaining points (open squares). The resulting light curve closely resembles those of hot spots: The eclipse is total, its ingress and egress are well defined, and the only obvious difference is that the luminosity of the superhump varies with time.

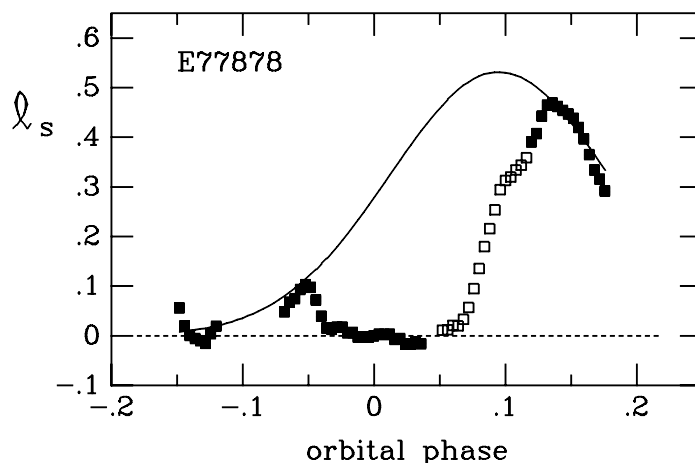


Fig. 7. The superhump eclipse light curve of E77878. See text for details.

We now use the four phases of contacts: $\phi = -0.05, -0.03, 0.06,$ and $0.12,$ to determine the location of SLS. For this purpose we employ the standard method used commonly (e.g. Wood et al. 1989) for hot spots. The result is shown in Fig.8. As we can see, the area defined by the four arches, representing the limb of the secondary in projection on the orbital plane at those four phases, coincides with the standard location of the hot spot at the intersection of the stream trajectory with the outer edge of the disk. This, incidentally, is consistent with earlier results of Warner and O'Donoghue discussed in the Introduction.

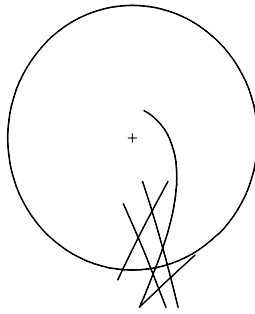


Fig. 8. Geometrical constraints on the location of SLS from eclipse E77878. Shown are: the disk, the stream trajectory, and short sections of the limb of the secondary (in projection on the orbital plane) at the four phases of contacts.

At this point we can explain the absence of the first minimum in the observed curve of E77878. This eclipse differs from the remaining ones in only one respect: it took place well before superhump maximum, i.e. at the time when absorption effects, due to the stream overflow, were – evidently – not yet present. This confirms the existence of an intrinsic connection between superhumps and the substantial stream overflow.

7. Conclusions

Evidence presented above leads to the following conclusions:

- (1) Superhumps are due to periodically enhanced dissipation of the kinetic energy of the stream resulting from strongly modulated mass transfer rate.
- (2) Substantial stream overflow occurs around superhump maximum making the superhump light source similar to "peculiar" spots observed at intermediate beat phases (cf. Smak 2007).

REFERENCES

- Hessman, F.V. 1999, *ApJ*, **510**, 867.
 Kunze, S., Speith, R., Hessman, F.V. 2001, *MNRAS*, **322**, 499.
 O'Donoghue, D. 1990, *MNRAS*, **246**, 29.
 Smak, J. 1994, *Acta Astron.*, **44**, 45.
 Smak, J. 2007, *Acta Astron.*, **57**, 87.
 Smak, J. 2008, *Acta Astron.*, **58**, 55.
 Warner, B., O'Donoghue, D. 1988, *MNRAS*, **233**, 705.
 Wood, J.H., Horne, K., Berriman, G., Wade, R.A. 1989, *ApJ*, **341**, 974.